Bolted T-stubs:
A refined model for flange and bolt fracture modes

Antonella B. Francavilla[*], Massimo Latour,
Vincenzo Piluso and Gianvittorio Rizzano

Department of Civil Engineering, Salerno University, Via Giovanni Paolo II, 132, 84084 Fisciano SA, Italy

Abstract. It is well known that, in order to accurately predict the behaviour of steel structures a requirement the definition of the mechanical behaviour of beam-to column joints is of primary importance. This goal can be achieved by means of the so-called component method, which, in order to obtain the whole behaviour of connections, provides to break up joints in basic components of deformability and resistance. One of the main joint components used to model bolted connections is the so-called equivalent T-stub in tension, which is normally used to predict the behaviour of bolted plates in bending starting from the behaviour of the single bolt rows. In past decades, significant research efforts have been devoted to the prediction of the behaviour of bolted T-stubs but, to date, no particular attention has been devoted to the characterization of their plastic deformation capacity. To this scope, the work presented in this paper, taking into account the existing technical literature, proposes a new theoretical model for predicting the whole behaviour up to failure of bolted T-stubs under monotonic loading conditions, including some complexities, such as the bolt/plate compatibility requirement and the bolt fracture, which are necessary to accurately evaluate the ultimate displacement. After presenting the advances of the proposed approach, a comparison between theoretical and experimental results is provided in order to verify its accuracy.

Keywords: bolted T-stubs; theoretical model; ductility; steel connections

1. Introduction

In past years, the actual behaviour of joints in steel structures was frequently disregarded and, normally, the structural behaviour was modelled by making the extreme assumptions of rigid or flexible behaviour (analysing continuous or pendular frames). Of course, these simplifications made structural calculations easier, but the structural model was not able to account for the actual behaviour of connections.

In the last few decades, the interest towards the prediction of the joint rotational behaviour in steel structures has significantly grown, as a consequence of the benefits deriving from the accuracy of such prediction. As a result, basing on the outcomes of many experimental and theoretical studies (Zoetemeijer 1974, Jaspart 1991, Girão Coelho *et al*. 2004a, b, Piluso *et al*. 2001, Bernuzzi *et al*. 1996, Faella *et al*. 2000, Latour *et al*. 2011b, Hantouche *et al*. 2012a, b, 2013, Lemonis and Gantes 2006, Takhirov and Popov 2002, Nair *et al*. 1974), modern codes have

---

∗Corresponding author, Ph.D. Student, E-mail: afrancavilla@unisa.it

introduced approaches aimed at the accurate prediction of the joint behaviour. In particular, the European methodology codified in last version of EC3 is based on the so-called component method (CEN 2005a, b), which consists in breaking up the joint in basic components contributing to the joint rotational deformability or resistance. Each component is separately modelled in terms of force-displacement or moment-rotation law and finally assembled in a mechanical model in order to obtain the whole joint behaviour.

Theoretically, this approach is very general and it is able to describe the behaviour of any kind of connection, provided that the basic components of deformability and strength are accurately identified and modelled. To date, even though the component method codified in EC3 is already very advanced and provides designers with significant information regarding the joint behaviour, it still provides some drawbacks especially dealing with the prediction of the plastic deformation capacity and of the cyclic behaviour. In fact, even though some authors have already investigated some aspects related to the prediction of the plastic deformation capacity (Latour and Rizzano 2013, Latour *et al*. 2014, Girão Coelho *et al*. 2004b, Beg *et al*. 2004) and of the cyclic behaviour of connections (Piluso and Rizzano 2008, Iannone *et al*. 2011, Latour *et al*. 2011a, Hu *et al*. 2012, Bravo and Herrera 2014), past experimental and theoretical researches have often focused their attention mainly on predicting stiffness and resistance of joints. Therefore, dealing with the prediction of the plastic deformation capacity of connections, at the present time, further efforts are still needed towards the codification in EC3 of a methodology for the prediction of the rotational capacity of joints.

In particular, in this paper, aiming to provide a contribution towards the codification of a procedure for the prediction of the plastic rotation capacity to be included in EC3, the attention is focused on bolted connections. In such connection typologies, usually, the most important components, such as the column flange or the end plate in bending, are modelled by means of equivalent T-stubs, i.e., two equal T-shaped elements connected through the flanges by means of one or more bolt rows. Therefore, in order to develop a theoretical approach for predicting the whole force-displacement response up to failure of bolted T-stubs, a new refined model is presented, starting from the existing literature.

To this scope, in this paper, the current state-of-the-art is presented and the assumptions and the theoretical framework are described, focusing the attention on the main advances of the proposed model. Successively, the constitutive laws adopted to define the behaviour of the materials composing plate and bolts (the sub-components of the T-stub) are described and the basic equations to derive, from the constitutive laws, the force-elongation response of bolts and the moment-rotation response of the plastic hinges forming on the T-stub flange plate are reported. Finally, the procedure adopted to assembly the sub-components of the T-stub in order to get the whole force-displacement response up to failure is described and a comparison with the experimental results is provided in order to evaluate the accuracy of the model. A particular attention is paid on to the prediction of the T-stub ultimate displacement.

2. Previous research

It is well known that the prediction of the force-displacement behaviour of bolted T-stubs is a complex matter, because its response is affected by many complicated phenomena, such as mechanical and geometrical non-linearities or contacts. As already said, to date, many attempts to model the structural behavior of T-stubs have been provided, but past researches have been mainly

focused on the prediction of stiffness and resistance, so that there are still some open issues especially dealing with the characterization of the T-stub plastic deformation capacity, which is a basic parameter in order to get the rotational capacity of bolted connections.

Historically, the problem of characterizing the force-displacement behaviour of bolted T-stub has been addressed by following mainly two approaches: the finite element or the mechanical modelling. In particular, in past years, finite element models have been largely applied both to structures and structural elements (Abidelah *et al.* 2014, Saberi *et al.* 2014). Nevertheless, even though, on one side, FE models allow to obtain very accurate predictions, on the other side, they need also the introduction of very detailed information regarding mechanical and geometrical non-linearities. Furthermore, they require specialized users and a high computational effort. Due to such reasons, in order to provide simpler and faster approaches, starting from the 60s also many simplified mechanical models have been presented by different authors. Looking back to past technical literature, models already available could be divided in: models for predicting the resistance (Yee and Melchers 1986, Zoetemeijer 1974, Douty and McGuire 1965, Swanson 2002, Reinosa *et al.* 2013), models for predicting the initial stiffness (Swanson 1999, Faella *et al.* 1998, Hantouche and Abboud 2014) and models for predicting the whole force-displacement curve of the T-stub up to failure (Jaspart 1991, Piluso *et al.* 2001, Swanson and Leon 2001).

The first attempts to define the mechanical behaviour of T-stubs have been proposed by (Zoetemeijer 1974, Douty and McGuire 1965, Yee and Melchers 1986). In a first work developed by (Douty and McGuire 1965), after investigating the effect of the material strain-hardening on the T-stub resistance, the authors proposed a simplified model for the strength prediction based on the adoption of the ultimate strength of the material composing the flange rather than on the yield stress. Successively, the role played by 3-D effects on the resistance of the T-stub (Zoetemeijer 1974) has been investigated. In particular, after presenting an approach based on the yield line method, the author found the expressions of the equivalent effective lengths. Practically, the approach presented (Zoetemeijer 1974) allows to use simplified beam models to obtain the T-stub resistance also for the cases where significant 3-D effects are expected. A methodology to define equivalent T-stubs for the column flange and end-plate to be used to model the behaviour of bolted connections has been also presented by (Yee and Melchers 1986). In addition, they proposed some empirical formulas calibrated on the available experimental tests able to predict the whole force-displacement behaviour of extended end-plate connections. Afterwards, models for predicting the resistance of the flange plate of T-stubs have been presented also in (Kulak *et al.* 1987) and (Jaspart 1991) which, with the previously cited work, represent the main theoretical basis of the expressions reported in EC3 part 1-8 (CEN 2005b). In particular, Kulak (Kulak *et al.* 1987) and Jaspart (1991) presented similar models based on simple translational and rotational equilibrium equations, whose main differences regard the assumptions made on the position and distribution of the forces under the bolt head and on the position of the plastic hinges arising on the flange plate. During the 90s significant work dealing with the prediction of stiffness and resistance of bolted T-stubs has been presented by other research (Swanson 1999, Piluso *et al.* 2001) facing also the issue of the prediction if the plastic deformation capacity. As advances of previous studies (Faella *et al.* 1998b; 2000, Swanson and Leon 2001, Swanson 2002), both authors presented a model for the prediction of the whole force-displacement behaviour of T-stubs able to predict the behaviour up to failure.

The approach proposed by Swanson (2001) is based on a multi-linear incremental model mainly developed for application into a computer program. In particular, such a model includes, even though in an approximate way, non-linear material properties, variable tension bolt stiffness

and elastic-plastic hinges to model the plate plasticity. Conversely, the limitations of the Swanson approach mainly regard the sensitivity to the strain-hardening parameters and to the bolt ductility, the approximations made to define the behaviour of the plastic hinges and the definition of the strain at failure of the materials composing the plate and the bolt which are not individuated using a standardized procedure. In addition, the bolt action is considered concentrated in one point consistently with the model proposed by Kulak (Kulak *et al*. 1987) and, therefore, the actual shape of the contact force distribution under the bolt head is not accounted for in the equilibrium equations.

The approach proposed by Piluso *et al*. (2001), still with some approximations, aims to provide a simple model to predict the force-displacement curve of the T-stub in line with Eurocode 3 and suitable for hand calculation. Such a model is based on the following hypothesis: geometrical non-linearities and 3-D effects are neglected, the compatibility between bolt and flange is disregarded as well as the shear interaction, prying forces are considered located at the tip of the flange plate and secondary flexural effects in the bolts are neglected. The procedure for obtaining the T-stub behaviour, in Piluso *et al*. (2001) model starts from the definition of the potential failure mode which is used to define the kinematic mechanism of the T-stub at collapse and the bending moment diagram arising on the flange plate. Afterwards, by making the hypothesis of fixed position of the point of zero-moment during the whole loading process, the behaviour of the plastic hinges arising on the flange plate is defined by means of the integration of the moment-curvature diagram of the rectangular cross-section representing the plate. Finally, the relationship between forces and displacements is evaluated by means of equilibrium equations and simple geometrical considerations. In addition, the failure of the T-stub is related to the ultimate rotation of the plastic hinges, which is defined as the rotation corresponding to the attainment of the plastic strain in the most extreme fibres of the section where the plastic hinge is located. The comparisons made versus the experimental tests show that the model of Piluso *et al*. (2001) is able to provide a very good approximation of the force-displacement curve if the failure mode of the T-stub is type-1, while it provides an underestimation of the resistance and an overestimation of the ductility supply if the failure mode is type-2 (as specified in the following sections). This is mainly due to the approximations the model makes with respect to the bolt. In fact, in the model, the compatibility between the elongation of the bolt and the deformation of the plate is neglected and, furthermore, the influence due to the bolt head size is not accounted for in the equilibrium equation.

More recently, a further model was presented (Girão Coelho *et al*. 2004b). Basically, it contains the same principles individuated by Swanson (2001) and Piluso (Piluso *et al*. 2001) for defining the behaviour of plate and bolts, but it introduces some complexities. In particular, the stress-strain relationship of the material composing the plate is modelled with a continuous law up to failure and the possibility of modelling the bolt action with a distributed load is considered. The comparisons made by the author show that the behaviour predicted by the model of Girão Coelho (2004b) is accurate in terms of resistance, but it reflects an overestimation of the plastic deformation capacity.

3. Main features of the proposed model

In general, the mechanical modelling of a T-stub can be provided starting from the definition of the geometry of the elements, the boundary conditions and the non-linear behaviour of its sub-components, i.e., the plate and the bolts.

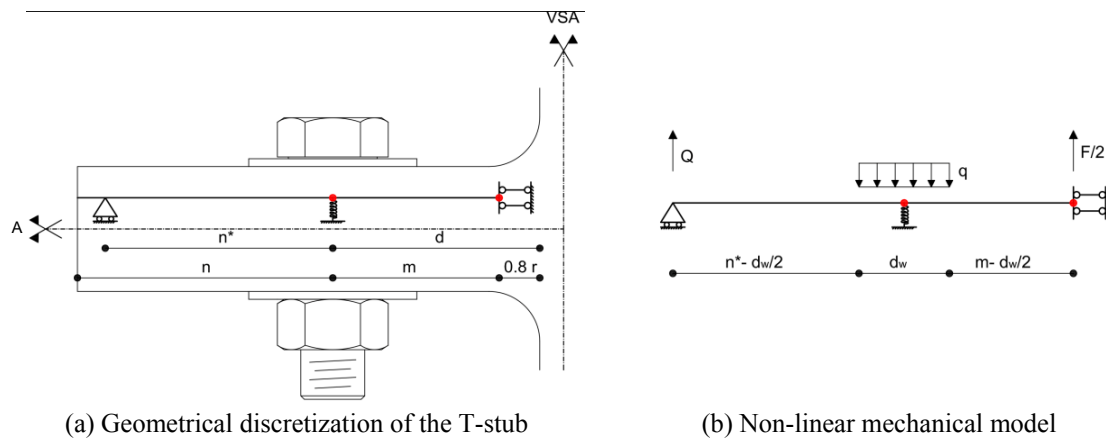(a) Geometrical discretization of the T-stub (b) Non-linear mechanical model

Fig. 1 T-stub model

The approach proposed in this paper aims to provide a modelling of the T-stub in line with the methodology already individuated by Eurocode 3. To this scope, the flange plate is modelled with a simplified beam, whose length is defined according to EC3 criteria, i.e., the distance between the bolt line and the plastic hinge arising at the T-stub stem is equal to $m = d - 0.8r$, while n is defined as the distance between the bolt line and the end of the plate (Fig. 1(a)). In order to model the influence of the bolt head on the resistance of the T-stub, which can provide a significant contribution to the resistance, the bolt action is assumed uniformly spread under the bolt head, over a length equal to the washer diameter (d_w) (Fig. 1(b)). At the same time, the bolt shank is modelled with a translational spring. Such a spring is defined in order to check the resistance of the bolt and to evaluate the respect of the compatibility condition between the elongation of the bolt and the deformation of the plate. Always in line with the EC3 approach, it is assumed that the beam composing the T-stub flange is constrained in correspondence of the stem, due to symmetry condition, with a bi-pendulum. To model the contact zone, as an advance on with respect to the existing models, the prying forces, which are usually assumed concentrated at the end of the plate, are considered applied in a point in between the tip of the plate and the edge of the bolt head. The position of such a point is determined by evaluating the compatibility of the vertical displacements of the plate in order to respect the horizontal symmetry condition.

The behaviour of the plate is defined adopting a lumped plasticity approach by means of non-linear plastic hinges located at the T-stub web and bolt line (Fig. 1). The characteristics of the plastic hinges are derived starting from the moment-curvature diagram of the cross-section representing the plate, according to the approach already presented by Piluso *et al.* (2001). In a similar way, also the non-linear spring modelling the bolt shank behaviour is characterized starting from the knowledge of the stress-strain law of the basic material according to the approach reported in the next section. The failure of the sub-components of the T-stub, i.e. the bolts and the plate, is modelled by checking the ultimate condition on the stress-strain laws of the materials. In particular, the failure of the plastic hinges of the plate is individuated as corresponding to the plastic rotation leading to the attainment ultimate strain at the most external fibre, while the failure of the bolt is identified in correspondence to the uplift value leading to the fracture elongation of the material composing the bolt.

In conclusion, still providing a simplified approach, the model proposed in this paper aims to define the response of the T-stub up to failure including the following advances:

● The bolt forces are considered uniformly distributed under the bolt head;
● The position of the contact forces is determined by evaluating the deformed configuration of the plate in the zone contained in between the bolt line and the tip of the plate;
● Mechanical non-linearities of plate and bolt are accounted for by means of integration of the stress-strain laws of the materials by extending the approach proposed by Piluso *et al.* for determining the moment-rotation response of the plastic hinges arising on the plate to the bolt force-elongation response;
● The failure of the T-stubs is modelled by checking the ultimate strain of the basic materials composing the plate and the bolts;
● The compatibility condition between the displacements of the plate and the uplift of the bolt is taken into account;
● The displacements of the T-stub are evaluated step-by-step as the sum of the elastic and plastic parts.

Despite these improvements, the following assumptions are still made:

● 3-D effects are neglected;
● Secondary bending effects on bolts are neglected;
● The effect of moment-shear interaction on resistance of the materials is neglected;
● The effect of shear forces in the bolts are neglected;
● Second order effects are neglected;
● The compatibility of the deformed shape of the plate in the zone contained between the prying force and the tip of the plate is not considered.

It is useful to note that, as far as 3-D effects are not considered, the model presented in this paper is mainly devoted to reproduce cases where the yield line pattern is the so-called beam pattern, which is, in practical cases, the pattern usually arising in T-stubs modelling the end-plates. In order to overcome this limitation, the model could be generalized also to other cases, at least for defining the resistance, by adopting the effective lengths already defined in (Zoetemeijer 1974). In addition, second order effects and shear forces in bolts are usually arising only at large displacements and therefore the model remains enough accurate in the range of sufficiently low displacements. In addition the effect of shear forces on the resistance of the materials are neglected and, therefore, in cases of T-stubs characterized by small values of the m/t_f ratio a slight overestimation of the resistance is expected.

3.1 Materials' constitutive laws

The plastic deformation capacity of steel plates strongly depends on the inelastic properties of the material and, above all, on the value of the ultimate strain. For this reason, in order to predict the ductility supply of T-stubs, an accurate modelling of the stress-strain relationships up to failure of the basic materials composing bolts and plate is necessary.

Preliminarily, it is useful to note that a conventional stress-strain relationship measured in common tensile tests is not representative of the punctual behaviour of the material. In fact, as it is well known, during a tensile test, the engineering stress σ_n, defined as the ratio between the force measured during the test (N) and the initial area of the specimen (A_0), after necking, starts to decrease due to the reduction of the cross-sectional area of the specimen. Notwithstanding, after

the beginning of necking, the true (natural) stress σ_r referred to the actual cross-sectional area A increases and the relationship between true stress and true strain of steel always follows an hardening behaviour up to failure.

Therefore, normally, in order to get the true stress–true strain behaviour starting from the results of coupon tensile tests, in the range before the necking phenomenon starts, it is necessary to transform the engineering values of stress and strain in actual values by means of the following relationships (Malvern 1969, Pozzati 1980, Davids *et al.* 1982)

$$\varepsilon_r = \ln \left(1 + \varepsilon_n\right); \quad \sigma_r = \sigma_n \left(1 + \varepsilon_n\right) \tag{1}$$

where ε_r is the actual (material) strain and ε_n is the nominal strain. In addition, in order to define the behaviour of the material in the range after necking up to failure, it is necessary to evaluate the ultimate natural stress σ_f at fracture and the corresponding natural deformation ε_u (RILEM 1990) by means of the following expressions

$$\sigma_f = \frac{F_f}{A_f}; \quad \varepsilon_u = \ln \frac{A_0}{A_f} \tag{2}$$

where F_f is the force measured by the testing machine at fracture and A_f is the area in the necking zone at the end of the test. The relationships here reported can be applied to obtain the actual stress-strain behaviour of steel provided that the results of coupon tensile tests are available. Such tests, are usually carried out only for the plates but not for the bolts some simplifying assumptions concerning the bolt material modelling have to be made.

The material composing the flange plate, as far as the results on coupon tensile tests are available, can be modelled in terms of actual strain vs. actual stress by means of a quadri-linear approximation, which can be derived starting from the experimental results by simply equating the area under the experimental curve with the area under the simplified quadri-linear curve (Fig. 2(a)).

Conversely, the material composing the bolts is not easy to accurately characterize as far as no experimental results are usually available. Nevertheless, bolt elongation is very important for the prediction of the ductility of joints. In fact, it may increase significantly the ultimate plastic deformation, allowing the uplift of the plate, in case of mechanisms type-2 or type-3. Also in

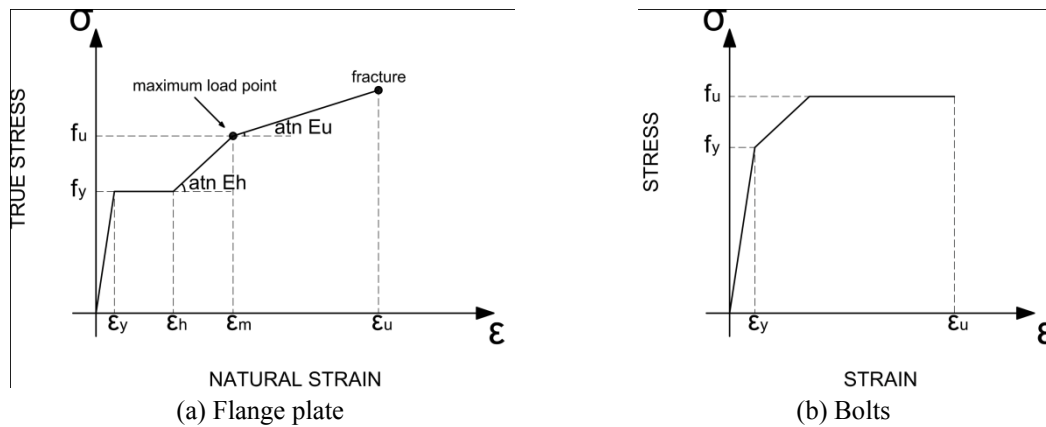(a) Flange plate   (b) Bolts

Fig. 2 Stress-strain laws of the materials composing the T-stub

EC3 no information is given with reference to the ultimate displacement of bolts and, since bolts are designed to remain in elastic range, in technical literature there are only few studies dealing with the characterization of the ultimate deformation of bolts. Within a wide experimental program dealing with the assessment of the behaviour of isolated T-stubs subjected to tension, four series of tests on high strength bolts axially loaded have been carried out (Girão Coelho *et al*. 2004a). The average ultimate deformation resulting from experimental tests indicated by the authors for short-threaded bolts of 8.8 and 10.9 class, is contained in the range 0.11-0.13. Other research, in a work devoted to propose a model to predict the ductility supply of joints, the authors indicated a value of the ultimate bolt deformation capacity equal to 0.1 (Beg *et al*. 2004).

Considering that, in technical literature, there is a common approach and usually the tests on the material composing the bolts used in the T-stub specimens are not available, in this work a simplified approach based on the application of an approximate tri-linear law is adopted (Fig. 2(b)). In particular, the proposed simplified tri-linear law is defined starting from the knowledge of the average values of the yield and ultimate stress of the material composing the bolt (i.e., for bolts class 8.8 [CoV = 0.07]: $f_{y,ave}$ = 723 MPa, $f_{u,ave}$ = 904 MPa; bolts class 10.9 [CoV=0.02]: $f_{y,ave}$ = 930 MPa, $f_{u,ave}$ = 1034 MPa), the stiffness of the second branch, which is characterized by a value of the Young modulus equal to 0.1E (Leon and Swanson 2000) and from the ultimate strain of the bolts. Such a strain value, since there are no specific indications in technical literature, is assumed equal to the elongation at fracture provided by the manufacturer of the bolts. This value, according to the manufacturer may vary in a minimum/maximum range according to prescribed values of the coefficient of variation. In particular, it is assumed that for bolt class 8.8, CoV = 0.1, A_{min} = 0.12, A_{max} = 0.18, while for bolt class 10.9, CoV = 0.1, A_{min} = 0.09, A_{max} = 0.14 (Fontana 2004).

3.1.1 Flexural behavior of the flange plate

Classically, the failure mechanisms of a bolted T-stub is dependent on the resistance of the composing elements, i.e. the bolts and the plate. In particular, in failure mechanism type-1, which is the most ductile as it provides the formation of significant plastic deformations in the flange plate under bending, the collapse is due to the formation of four plastic hinges contemporarily arising in correspondence of the flange-to-web connection and bolt line. Conversely, in failure mechanism type-3, the failure mechanism is characterized only by the bolt collapse. Finally, failure mechanism type-2 is intermediate between mechanisms type-1 and type-3, as it provides the collapse of the T-stub due to the failure of the bolt or of the flange plate due to the attainment of the ultimate rotation of the plastic hinges arising at the flange-to-web connection (Fig. 3).

Considering the classical definition of failure modes and their kinematic mechanisms, it is clear that, in order to accurately predict the complete behaviour of a bolted T-stub, first of all, it is important to accurately define both the rotational capacity of the plastic hinges arising in the flange plate and the force-elongation relationship for the bolt. In fact, in case of mechanism type-1, as the collapse is due to the plate failure, the behaviour and the ductility capacity of the T-stub mainly depends on the ability of the plastic hinges to rotate and, in particular, on their moment-rotation response, while, in case of mechanism type-3, as failure is governed by bolts, it mainly depends on their force-elongation response. Obviously, in case of mechanism type-2, which is intermediate between mechanism type-1 and type-3, both the rotational response of the plastic hinges and the force-elongation response of bolts are of concern, because in this case the failure of the bolt or of the plate mainly depends on the relative resistance and ductility of the two components.

In particular, in the proposed model the plate behaviour is characterized by following an approach similar to that already provided in (Piluso *et al*. 2001). Within this approach, the
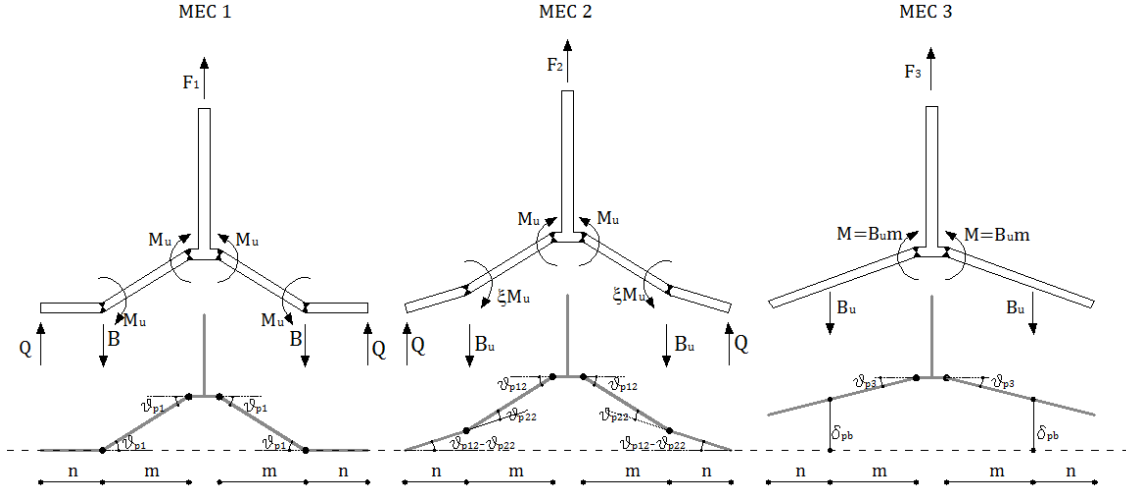
Fig. 3 Classical definition of the failure modes

moment-rotation behaviour of the plastic hinges is derived passing from the true stress-true strain response of the basic material composing the plate to the moment-curvature relationship of the plate and, afterwards, it is obtained by means of integration of the curvatures along the plate.

Moment–curvature relationship

Following the same methodology provided by (Piluso *et al.* 2001), the behaviour of the plastic hinges arising on the flange plate is defined starting from the moment-curvature M-χ relationship of the rectangular cross-section representing the flange plate. Such a relationship assumes four different mathematical laws in correspondence of the boundary strains ε_y, ε_h, ε_m, ε_u (Fig. 2(a)). Under the hypothesis of pure bending, the significant values of the curvatures can be defined as

$$\chi_y = \frac{2\varepsilon_y}{t_f} \qquad \chi_h = \frac{2\varepsilon_h}{t_f} \qquad \chi_m = \frac{2\varepsilon_m}{t_f} \qquad \chi_u = \frac{2\varepsilon_u}{t_f} \tag{3}$$

where t_f is the flange plate thickness. For each one of these curvature values, by writing the equilibrium equations the following branches, expressed in terms of non-dimensional bending moment vs non-dimensional curvature $M/M_y - \chi/\chi_y$, can be obtained:

- Elastic Branch ($\chi/\chi_y < 1$):

$$\frac{M}{M_y} = \frac{\chi}{\chi_y} \tag{4}$$

- Yield Plateau ($1 < \chi/\chi_y < \chi_h/\chi_y$):

$$\frac{M}{M_y} = \frac{1}{2}\left[3 - \left(\frac{\chi_y}{\chi}\right)^2\right] \tag{5}$$

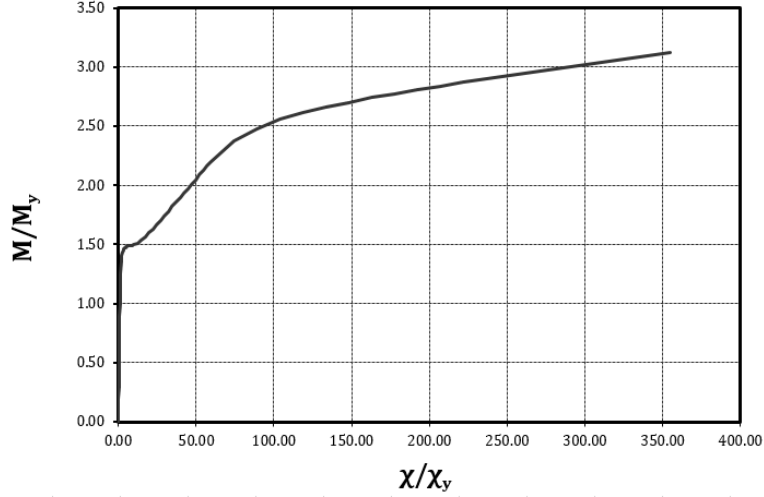- Hardening Branch ($\chi_h/\chi_y < \chi/\chi_y < \chi_m/\chi_y$):

Fig. 4 Example of non-dimensional moment-curvature diagram

$$\frac{M}{M_y} = \frac{1}{2}\left[3 - \left(\frac{\chi_y}{\chi}\right)^2\right] + \frac{1}{2}\frac{E_h}{E}\left(\frac{\chi - \chi_h}{\chi_y}\right)\left(1 - \frac{\chi_h}{\chi}\right)\left(2 + \frac{\chi_h}{\chi}\right) \tag{6}$$

- Post-necking ($\chi_m/\chi_y < \chi/\chi_y < \chi_u/\chi_y$):

$$\frac{M}{M_y} = \frac{1}{2}\left[3 - \left(\frac{\chi_y}{\chi}\right)^2\right] + \frac{1}{2}\frac{E_h}{E}\left(\frac{\chi - \chi_h}{\chi_y}\right)\left(1 - \frac{\chi_h}{\chi}\right)\left(2 + \frac{\chi_h}{\chi}\right) +$$
$$-\frac{1}{2}\frac{E_h - E_u}{E}\left(\frac{\chi - \chi_m}{\chi_y}\right)\left(1 - \frac{\chi_m}{\chi}\right)\left(2 + \frac{\chi_m}{\chi}\right) \tag{7}$$

where $M_y = (bt_f^2/6)f_y$ is the T-stub width and f_y is the material yield stress. From the previous equations, it is useful to observe from previous equations that the M_h/M_y, M_m/M_y, M_u/M_y ratios depend only on the properties of the material composing the flange plate (Fig. 4).

Moment-rotation behaviour of the plastic hinges

By exploiting the definition of the moment-curvature relationships, the moment-rotation curves of the plastic hinges modelling the non-linear behaviour of the T-stub flange plate can be determined. Following the same approach provided by Piluso *et al*. (2001) such plastic rotations can be evaluated by means of the following steps:

- Evaluation of the bending moment diagram along the T-stub flange;
- Definition of the curvatures along the flange plate by inverting the moment-curvature relations previously defined;
- Integration of the curvatures on single cantilever beams in order to obtain the rotations of the plastic hinges.
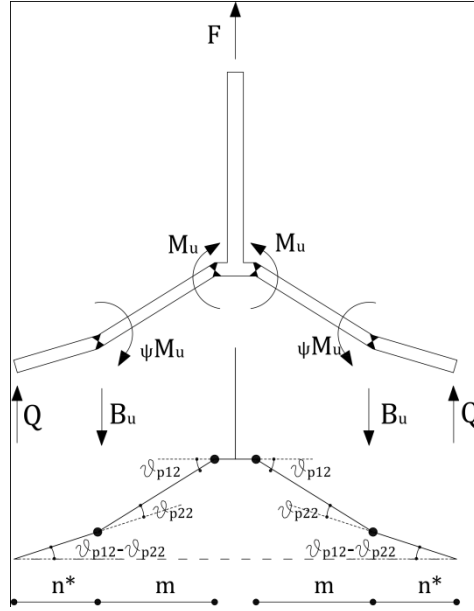
Fig. 5 Assumed kinematic collapse mechanism

The diagram of the bending moment arising on the T-stub flange plate is not known a priori and it depends on the system of equilibrium and compatibility equations to be solved according to the procedure reported in next section. Nevertheless, it is useful to note that the shape of such a diagram, in any point of the force-displacement T-stub curve, depends only on the applied loads and on the value of the bending moment arising in correspondence of the plastic hinges, whose ratio, consistently with the kinematic collapse mechanism reported in Fig. 5 can be defined as ψM_u.

Therefore, it is linear in the zone in between the plastic hinge arising at the web and the tip of the bolt head, parabolic in the zone of the bolt head and again linear in the zone contained in between the bolt head and the prying force (Fig. 6).

Following Piluso *et al.* (2001) approach, starting from the moment distribution arising along the T-stub flange depicted in Fig. 6, the mathematical laws defining the rotations of the plastic hinges can be obtained by considering, in a simplified way, the three simple cantilever schemes reported in Fig. 6, which are characterized by a maximum value of the bending moment equal to $M_1 = M$, $M_2 = M_3 = \psi M$ and lengths L_1, L_2 and L_3 equal to

$$L_1 = \frac{m}{1+\psi} \qquad L_2 = \frac{m\psi}{1+\psi} \qquad L_1 = n^* \tag{8}$$

Within this work, the parabolic part of the bending moment diagram is approximated with a linear segment internal to the actual diagram. This approximation is made in order to simplify the expressions of the mathematical laws providing the values of the rotations of the plastic hinges. It is worth observing that, this approximation leads to a slight overestimation of the rotation of the plastic hinge arising at the T-stub web ϑ_{p1} and a slight underestimation of the plastic rotation arising at the bolt line ϑ_{p2}.

Therefore, for each simple cantilever scheme, the value of the plastic rotation is obtained from
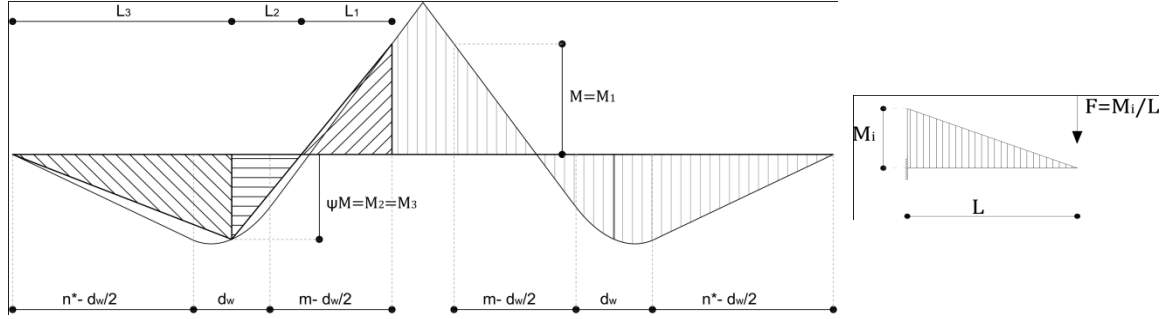
Fig. 6 Cantilever scheme for evaluating the plastic rotations

the inversion of the moment-curvature diagram reported in previous paragraph and the integration of the curvatures along the cantilever. Such an integration provides the values of the following functions already defined by Piluso *et al*. (2001):

Case 1: $\xi \leq \xi_1 = \dfrac{M_y}{M_u}$

$$\vartheta_p = 0 \tag{9}$$

Case 2: $\xi_1 < \xi \leq \xi_2 = \dfrac{M_h}{M_u}$

$$\vartheta_p = \frac{L}{t_f} D(\xi) \tag{10}$$

Case 3: $\xi_2 < \xi \leq \xi_3 = \dfrac{M_m}{M_u}$

$$\vartheta_p = \frac{L}{t_f} F(\xi) \tag{11}$$

Case 4: $\xi_3 < \xi \leq 1$

$$\vartheta_p = \frac{L}{t_f} G(\xi) \tag{12}$$

where ξ is equal to the ratio between the bending moment and M_u and the functions $D(\xi)$, $F(\xi)$ and $G(\xi)$ depend only on the mechanical properties of the plate. For the sake of clarity, the complete expressions of the functions are reported in the **Annex A** of this paper. A typical non-dimensional moment-rotation behaviour of the plastic hinge is delivered in Fig. 7.

With reference to the kinematic collapse mechanism reported in Fig. 5, it is easy to verify by means of geometrical considerations, that the plastic displacement of the T-stub can be expressed as a function of the plastic hinges rotation by means of the following relationship

$$\delta_{p,T-stub} = \vartheta_{p1} m + \left(\vartheta_{p1} - \vartheta_{p2}\right) n^* \tag{13}$$
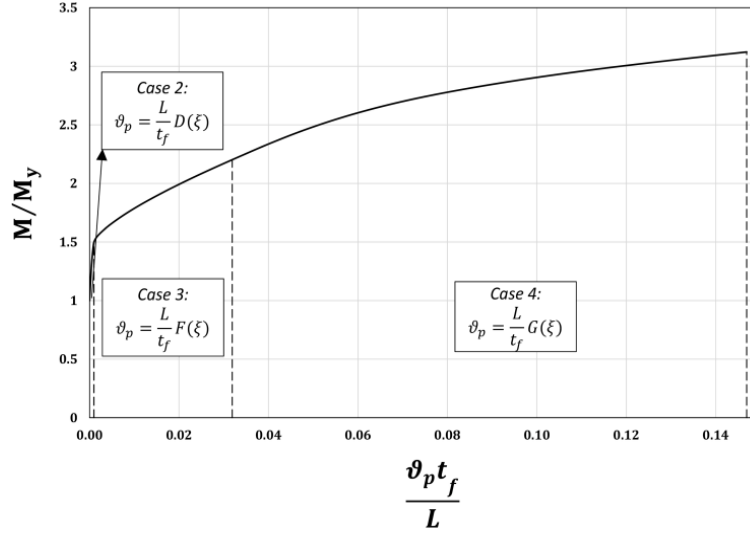
Fig. 7 Typical moment-rotation behavior of the plastic hinge

where ϑ_{p1} is the plastic rotation of the first cantilever scheme characterized by the length L_1 and the bending moment M_1; ϑ_{p2} is equal to the sum of the plastic rotations of the other two cantilever schemes defined in Fig. 6. In addition, due to compatibility requirements with the vertical displacement of the plate in the contact zone, ϑ_{p1} has to be greater than ϑ_{p2}, otherwise $\vartheta_{p1} = \vartheta_{p2}$.

3.1.2 Axial behavior of the bolt

As aforesaid, analogously to the flange plate, the force-elongation behaviour of the bolt can be characterized starting from the definition of the stress-strain law of the basic material. It is easy to understand that, in this case, the translational spring representing the bolt behaviour can be defined by multiplying the strains and the stresses of the constitutive law by the length (L_b) and the net section area (A_{res}) of the shank respectively. Consistently with the Eurocode 3 approach, the conventional length of the bolt can be defined as

$$L_b = 2t_f + \frac{t_n + t_{bh}}{2} + 2t_w \tag{14}$$

where t_n is the nut thickness, t_{bh} is the thickness of the bolt head and t_w is the thickness of the washer.

Therefore, the force-elongation behaviour of the bolt can be characterized by means of the following tri-linear behaviour:

- **1st Branch**: Elastic ($\delta \leq \delta_y$):

$$B = K_0 \cdot \delta \tag{15}$$

- **2st Branch**: Inelastic ($\delta_y < \delta \leq \delta_h$):

$$B = 0.10 \cdot K_0 \cdot \delta \tag{16}$$

- **3st Branch**: Plateau ($\delta > \delta_h$):

$$B = B_u \tag{17}$$

where the contribution of the initial stiffness of the bolt, with reference to the single tee element, is equal to

$$K_0 = \frac{2EA_{res}}{L_b} \tag{18}$$

while the boundary displacements, dividing the different branches are

$$\delta_y = \frac{f_y L_b}{2E}$$

$$\delta_h = \delta_y + \frac{\left(B_u - B_y\right)}{0.10 K_0} \tag{19}$$

$$\delta_u = \varepsilon_u L_b$$

Finally, the yielding and ultimate bolt forces are given by

$$B_y = A_{res} \cdot f_y$$
$$B_u = A_{res} \cdot f_u \tag{20}$$

4. Model assembling

As far as the basic assumptions and the mathematical laws defining the non-linear behaviour of flange plate and bolt are defined, it is possible to define the procedure to assembly the sub-components of the T-stub (i.e., the plate and the bolt) in order to get the whole force-displacement curve up to failure. According to the assumptions made and to the bending moment distribution depicted in Fig. 6, for a fixed value of the bending moment $M_j = M_1$ acting in correspondence of the T-stub web, there are five unknown parameters (Fig. 1(b)). The force transmitted through the T-stub web (F), the prying force (Q), the value of the distributed load corresponding to the action provided by the bolt head (q), the ratio between the bending moment acting at the bolt line and that arising at the T-stub web (ψ) (Fig. 6) and the location of the prying forces in the contact zone (n^*). In order to solve the problem, five equations can be written: the translational equilibrium, the rotational equilibrium around the plastic hinge located in correspondence of the web, the rotational equilibrium of the left portion of the plate beam around the point of application of the bolt force, the compatibility equation between the T-stub flange and the elongation of the bolt at the bolt line and the compatibility equation of the vertical displacements in the contact zone. Therefore, the system of equations to be solved, in its general form, can be written as follows:

$$\begin{cases} \dfrac{F}{2} + Q - qd_w = 0 \\[2mm] Q\left(m + n^*\right) - qd_w m + M_j = 0 \\[2mm] Qn^* - \dfrac{qd_w^2}{8} - \psi M_j = 0 \\[2mm] \delta_{b.e;} + \left[\vartheta_{p1}(\psi) - \vartheta_{p2}(\psi)\right]n^* = \dfrac{qd_w}{K_{sec}} \\[2mm] \left\{ v_1(z_1) + \left[\vartheta_{p1}(\psi) - \vartheta_{p2}(\psi)\right]z_1 \right\}_{min} > 0 \end{cases} \qquad (21)$$

where $\delta_{b,el}$ is the elastic part of the vertical displacement evaluated at the bolt line, K_{sec} is the value of the bolt secant stiffness determined on the force-elongation curve previously defined, $\vartheta_{p1}(\psi)$ and $\vartheta_{p2}(\psi)$ are the plastic rotations of the hinges to be evaluated according to the procedure previously reported, whose values depend on the parameter ψ, $v_1(z_1)$ is the distribution of the plate elastic displacements in the contact zone and z_1 is the value of the abscissa starting from the tip of the plate.

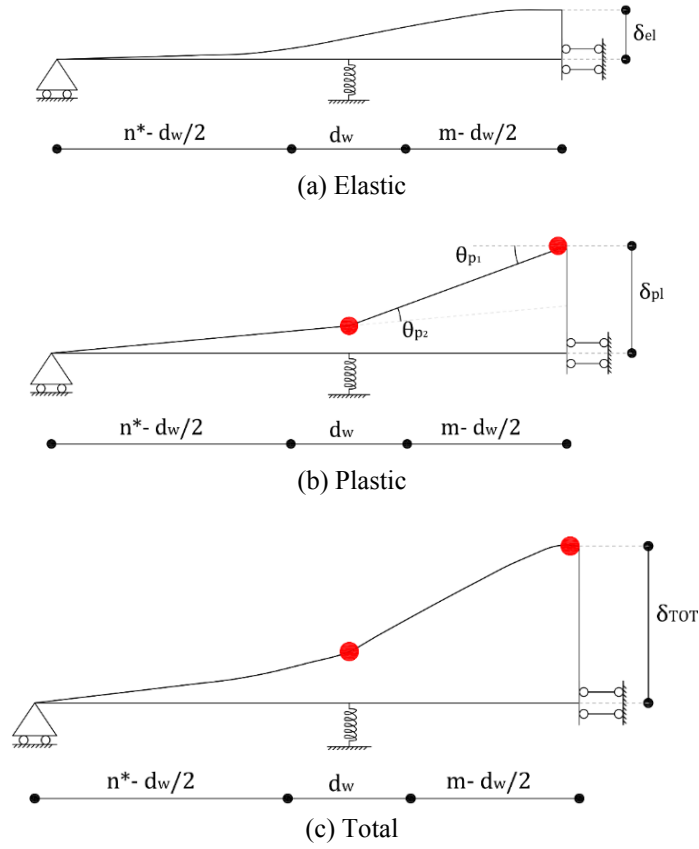(a) Elastic

(b) Plastic

(c) Total

Fig. 8 Deformed shape of the flange

It is worth noting that fourth and fifth equation of system (21) depend on the elastic part of the plate displacement (Fig. 8(a)) and, due to this reason, it is necessary to define the mathematical laws of the vertical deflections of the plate in a closed form. To this scope, the static beam equations for the three portions $0 \leq z_1 \leq n^* - d_w/2$, $0 \leq z_2 \leq d_w$ and $0 \leq z_3 \leq m - d_w/2$ have been written imposing appropriate boundary conditions. For the sake of clarity, the solutions providing the deflections of the plate, are reported in **Annex B**.

Observing Eq. (21), it is easy to understand that the solution of the system is untrivial in a closed form. In fact, the equations providing the expressions of the flange plate plastic rotation are quite complicated (Annex A) and, in addition, the point where the prying force is applied is not directly evaluable because it depends on the expression of the vertical deflection of the plate in the contact zone (Annex B).
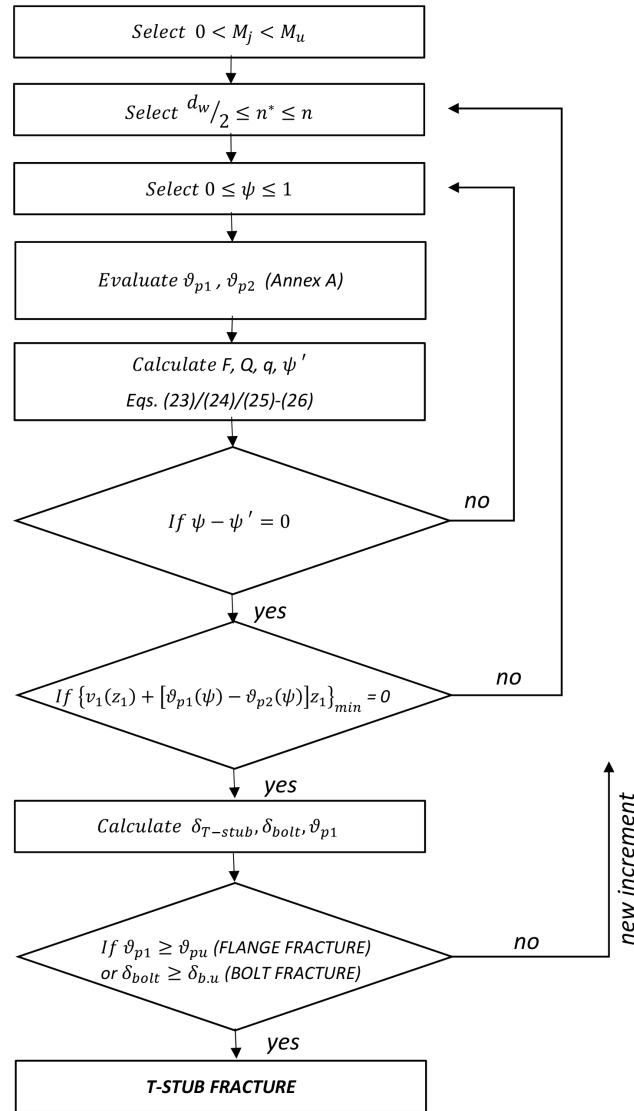

Fig. 9 Flow-chart for solving the system of Eq. (21)

Nevertheless, the system can be solved incrementally by means of the algorithm reported in Fig. 9. In particular, following this algorithm, for every assigned value of the bending moment M_j, the system of equations can be iteratively solved by preliminarily fixing n^* and an attempt value of ψ in order to determine ϑ_{p1} and ϑ_{p2} and, from the first four equations of the system, the values of q, F, Q, and a new value $\psi = \psi'$ of the parameter, providing the bending moment of the bolt axis. In particular, q can be calculated from the following equations, whose application range depends on the deformation state of the bolt:

Case 1 – Bolt in the elastic range

$$q_1 = \frac{64 K_0 n^* \left[3m^2 M_j + 6 M_j m n^* + 2 M_j n^{*2} + 6 EI \left(\vartheta_{p1-} \vartheta_{p2} \right) \left(m + n^* \right) \right]}{d_w \left\{ 192 EI \left(m + n^* \right) + K_0 \left[d_w^2 \left(m + n^* \right) - 16 d_w^2 n^* \left(m + n^* \right) + 64 m n^{*2} \left(3m + 2n^* \right) \right] \right\}} \tag{22}$$

Case 2 – Bolt in the plastic range

$$q_2 = 0.1 \cdot q_1 + 0.9 \cdot \frac{B_y}{d_w} \tag{23}$$

Case 3 – Bolt in the plateau range

$$q_2 = 0.1 \cdot q_1 + 0.9 \cdot \frac{B_y}{d_w} \tag{24}$$

while F, Q and ψ' can be calculated by exploiting the following relationships

$$F = 2 \frac{\left(q d_w n^* + M_j \right)}{m + n^*}$$

$$Q = \frac{\left(q d_w m - M_j \right)}{m + n^*} \tag{25}$$

$$\psi' = \frac{q d_w \left[d_w \left(m + n^* \right) - 8 m n^* \right] + 8 M_j n^*}{8 M_j \left(m + n^* \right)}$$

Afterwards the accuracy of the solution can be evaluated by checking the respect of last equation of the system and the difference between ψ and ψ'.

As far as the force-displacement curve of the T-stub is obtained by progressively increasing the bending moment acting on the flange, at the end of each loading step it is possible to check also for the deformation state of plastic hinges and bolt. In this way it is possible to control if the rotations and the elongations are compatible with the plastic deformation capacity provided by the basic materials.

In order to verify the accuracy of the model, the authors have developed a specific program based on the reported algorithm in Visual Basic for Application.

5. Comparison with experimental results

In order to evaluate the accuracy of the theoretical model, some comparisons with the experimental tests already carried out at Laboratory of Materials and Structures of the Department of Civil Engineering of Salerno University (Piluso *et al*. 2001) have been considered. The tests concern eleven specimens fabricated by coupling T-stubs obtained from hot-rolled profiles of HEA and HEB series and one specimen obtained by welding two plates according to a T-shape.

With reference to the notation given in Fig. 10, the measured values of the geometrical properties of tested specimens are reported in Tab.1. The value of r provided for specimen-12 (the welded T-stub) corresponds to the value of the throat thickness of the weld connecting the T-stub web to the flange.
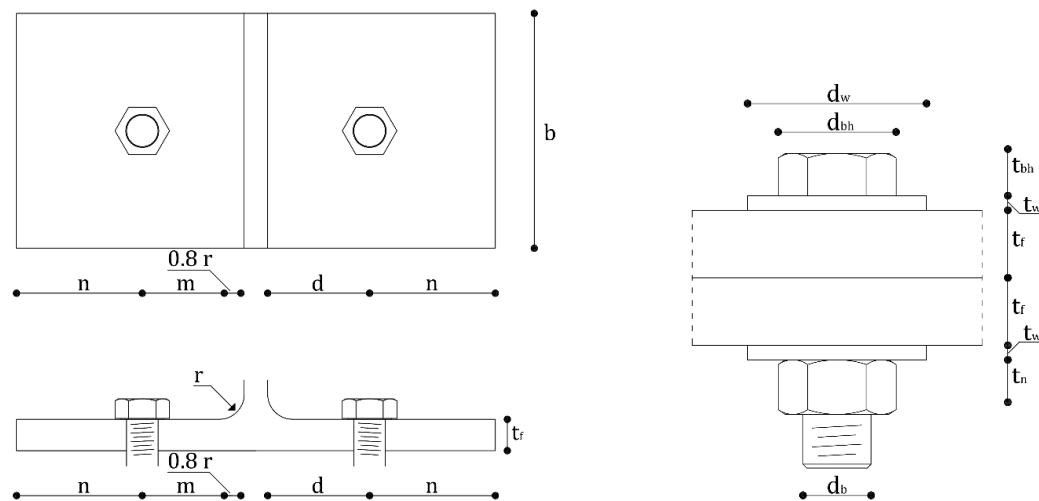

Fig. 10 Geometrical configuration of the specimens

Table 1 Geometrical properties of tested specimens (Piluso *et al*. 2001)

T-stub	1	2	3	4	5	6	7	8	9	10	11	12
d_b (mm)	20.00	20.00	20.00	24.00	24.00	24.00	27.00	24.00	27.00	20.00	20.00	20.00
d_h (mm)	33.53	33.53	33.53	39.98	39.98	39.98	45.20	39.98	45.20	30.00	33.53	33.53
d_w (mm)	37.00	37.00	37.00	44.00	44.00	44.00	56.00	44.00	56.00	37.00	37.00	37.00
t_{bh} (mm)	12.72	12.72	12.72	14.78	14.78	14.78	17.35	14.78	17.35	12.72	12.72	12.72
t_n (mm)	16.00	16.00	16.00	19.00	19.00	19.00	27.00	19.00	27.00	16.00	16.00	16.00
t_f (mm)	14.40	14.60	13.00	12.30	13.80	16.3	13.90	13.30	12.50	10.85	9.50	12.20
t_w (mm)	4.00	4.00	4.00	4.00	4.00	4.00	4.00	4.00	4.00	4.00	4.00	4.00
m (mm)	39.30	39.30	42.30	48.95	49.75	45.65	52.45	45.20	54.05	32.60	36.40	53.50
n (mm)	40.80	40.80	22.20	58.10	74.90	45.20	71.70	19.30	53.00	58.50	38.00	49.90
r (mm)	18.00	18.00	15.00	24.00	27.00	18.00	27.00	15.00	24.00	18.00	15.00	7.50
b (mm)	126.50	119.00	124.00	118.80	115.00	120.00	122.80	112.50	125.10	125.00	159.00	90.25

Table 2 Mechanical properties of tested specimens (Piluso *et al.* 2001)

T-stub	1	2	3	4	5	6	7	8	9	10	11	12
f_y (MPa)	291.16	264.95	273.15	299.76	317.72	280.46	307.58	269.42	300.97	293.10	324.33	346.50
f_u (MPa)	517.21	501.11	504.33	543.59	546.84	527.76	543.57	482.70	552.27	514.87	530.93	460.77
E_h (MPa)	3276	3171	3087	2877	3339	3360	3423	3276	3234	2163	2184	2310
E_u (MPa)	371.11	378.32	435.95	465.24	483.15	488.11	516.05	476.80	466.65	406.32	347.93	383.02
ε_h (%)	1.358	1.135	1.171	1.285	1.362	1.202	1.318	1.055	1.290	0.600	2.040	0.870
ε_u (%)	49.18	48.12	58.70	76.77	78.43	63.83	77.88	69.40	67.75	92.50	96.98	95.29
f_{ub} (MPa)	904	904	904	904	904	904	904	904	904	1034	904	904

The mechanical properties of the materials composing the flange plates of the specimens have been obtained in terms of true stress-true strain starting from the results of coupon tensile tests (Table 2).

For all the specimens, the proposed mechanical model has been applied and compared with the corresponding experimental results (Fig. 11). In particular, in the graphs, the predicted curves are represented by indicating three displacement values corresponding to the attainment of: (1) the bolt fracture calculated by considering the lower limit of the elongation at break suggested by the producer (bolt class 8.8/10.9, $A_{min} = 0.12/0.09$); (2) the bolt fracture calculate by considering the upper limit of the elongation at break suggested by the producer (bolt class 8.8/10.9, $A_{min} = 0.18$
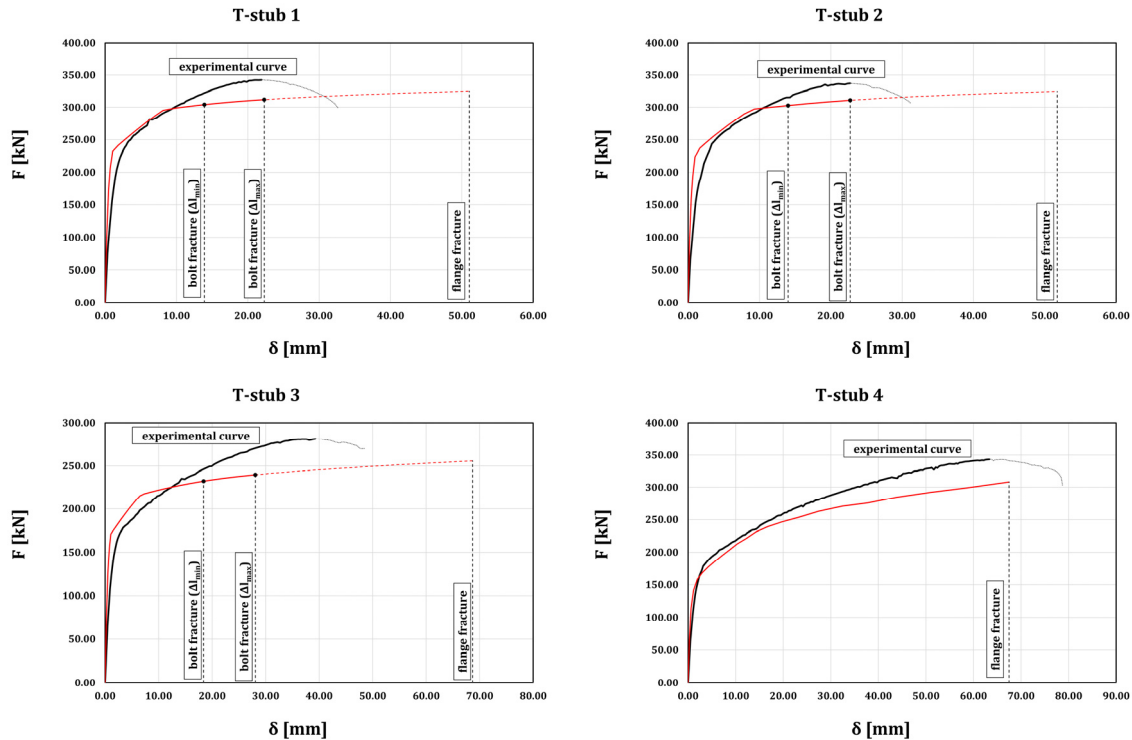

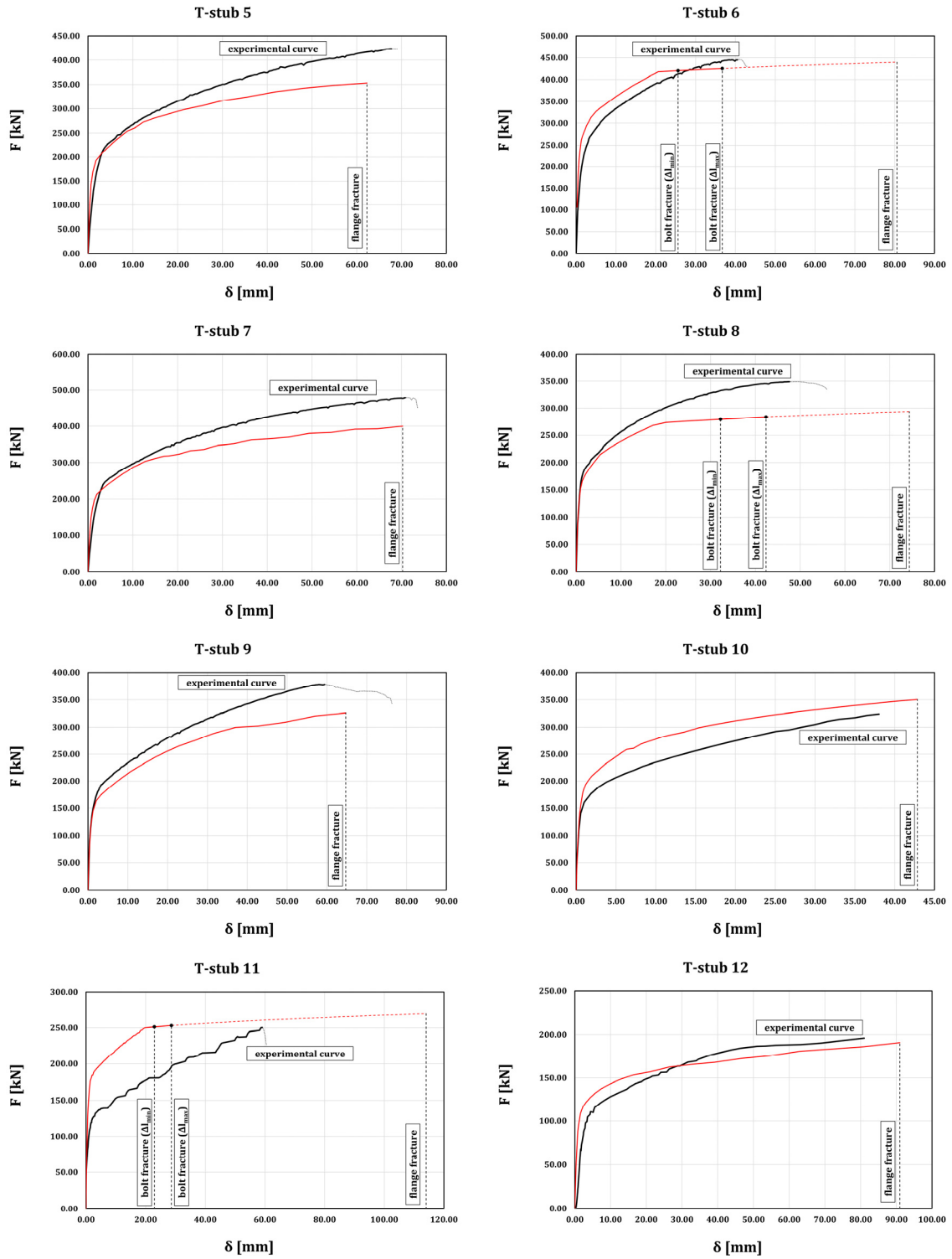Fig. 11 Comparison between experimental results and theoretical predictions

Fig. 11 Continued

Table 3 Mechanical model vs Experimental tests

T-stub	1	2	3	4	5	6	7	8	9	10	11	12
$\delta_{u,exp}$ (mm)	21.91	22.71	39.3	63.71	68.16	40.80	70.81	47.61	59.41	38.03	59.08	81.00
δ_{u,th_min} (mm)	13.91	14.01	18.41	-	-	25.59	-	32.24	-	-	39.25	-
δ_{u,th_max} (mm)	22.30	22.72	28.08	-	-	36.70	-	42.38	-	-	63.18	-
$\delta_{u,th}$ (mm)	18.11	18.37	23.24	67.49	62.27	31.25	70.24	37.31	64.73	42.84	51.22	90.97
$\delta_{u,th}/\delta_{u,exp}$	0.83	0.81	0.59	1.06	0.91	0.76	0.99	0.78	1.09	1.13	0.87	1.12
$F_{u,exp}$ (kN)	342.39	337.14	281.46	343.32	423.61	445.76	479.40	348.75	378.01	323.81	250.41	195.95
F_{u,th_min} (kN)	304.21	302.76	232.09	-	-	420.18	-	279.36	-	-	278.22	-
F_{u,th_max} (kN)	311.96	310.89	239.46	-	-	425.05	-	283.46	-	-	299.22	-
$F_{u,th}$ (kN)	308.09	305.49	235.78	308.27	353.09	422.61	399.56	281.41	325.81	350.27	288.72	190.80
$F_{u,th}/F_{u,exp}$	0.90	0.91	0.84	0.90	0.83	0.95	0.83	0.81	0.86	1.08	1.15	0.97

Table 4 Main results obtained by solving the system of Eq. (21)

T-stub	1	2	3	4	5	6	7	8	9	10	11	12
ϑ_{p1}	0.114	0.115	0.179	0.663	0.617	0.206	0.662	0.313	0.593	0.644	0.251	0.842
ϑ_{p2}	0.002	0.003	0.001	0.621	0.591	0.068	0.636	0.088	0.559	0.615	0.116	0.816
ψ'	0.516	0.536	0.469	0.834	0.799	0.635	0.818	0.695	0.863	0.756	0.764	0.866
Q [kN]	67.154	67.96	103.313	116.415	80.362	111.005	126.384	178.280	169.108	56.495	101.951	86.528
q [kN]	5.987	5.987	5.987	6.149	5.892	7.250	5.859	9.016	5.955	6.277	6.159	4.921
n^* [mm]	40.800	40.800	22.200	35.720	59.031	42.881	47.667	19.300	31.751	54.501	25.132	32.631

/0.14); (3) the flange fracture.

The comparisons of the model with the experimental tests show a very satisfactory agreement in terms of shape of the force-displacement curve and in terms of prediction of the plastic deformation capacity.

In particular, in Table 3, the predicted values of the T-stub displacement capacity and ultimate resistance have been compared with the experimental ones in terms of ratio $\delta_{u,th}/\delta_{u,exp}$ and $F_{u,th}/F_{u,exp}$. Dealing with the prediction of the displacement capacity, the mean value of ratio $\delta_{u,th}/\delta_{u,exp}$ is equal to 0.91 with a standard deviation equal to 0.17. Conversely, dealing with the T-stub ultimate resistance, the mean value of the ratio $F_{u,th}/F_{u,exp}$ is equal to 0.92 with a standard deviation equal to 0.11. This results correspond to a slight underestimation of the resistance and ductility supply of the T-stub. Nevertheless, the obtained results are almost always on the safe side. For the sake of clarity, in Table 4, the value of the parameters ϑ_{p1}, ϑ_{p2}, ψ', q and n^* are summarized for all the experimental tests simulated.

6. Conclusions

Starting from an analytical model previously developed, a refined model to analyse the whole force-displacement curve of bolted T-stubs has been proposed. The basic assumptions and the governing equations, whose solution requires a non-linear incremental procedure, have been also

presented.

The accuracy of the proposed model has been investigated by means of a comparison with twelve experimental tests, both in terms of resistance and of plastic deformation capacity.

The results obtained are satisfactory and on safe side. In fact, regarding the prediction of the ultimate resistance, the average ratio between the value predicted by the model and the experimental one is equal to 0.92. Similarly, the ratio between the predicted ultimate displacement and the experimental value is equal to 0.91. These results, compared to the complexity of the analysed connection component, are enough accurate for practical application. In particular, it has to be underlined that the model allows to predict with sufficient accuracy the plastic deformation capacity of bolted T-stubs which is currently not covered by codified rules. Therefore, the model can be effective in providing a safe side estimation of the plastic rotation capacity of extended end-plate connections as the ratio between the ultimate plastic deformation of the end-plate component at the tensile flange level (modelled by means of an equivalent T-stub) and the level arm.

References

Abidelah, A., Bouchair, A. and Kerdal, D. (2014), "Influence of the flexural rigidity of the bolt on the behavior of the T-stub steel connection", *Eng. Struct.*, **81**, 181-194.

Beg, D., Zupancic, E. and Vayas, I. (2004), "On the rotation capacity of moment connections", *J. Construct. Steel Res.*, **60**(3-5), 601-620.

Bernuzzi, C., Zandonini, R. and Zanon, P. (1996), "Experimental analysis and modelling of semi-rigid steel joints under cyclic reversal loading", *J. Construct. Steel Res.*, **38**(2), 95-123.

Bravo, M. and Herrera, R. (2014), "Performance under cyclic load of built-up T-stubs for double T moment connections", *J. Construct. Steel Res.*, **103**, 117-130.

CEN (2005a), Eurocode 3: Design of steel structures - Part 1-1: General rules and rules for buildings, s.l.:s.n.

CEN (2005b), Eurocode 3: Design of steel structures - Part 1-8: Design of joints, s.l.:s.n.

Davids, E., Troxell, G. and Hanck, G. (1982), *The Testing of Engineering Materials*, McGraw-Hill, New York, NY, USA.

Douty, T. and McGuire, W. (1965), "High strength bolted moment connections", *J. Struct. Div.*, **91**(2), 101-128.

Faella, C., Piluso, V. and Rizzano, G. (1998), "Experimental analysis of bolted connections: Snug versus preloaded bolts", *J. Struct. Eng.*, **124**(7), 765-774.

Faella, C., Piluso, V. and Rizzano, G. (2000), *Structural Steel Semi-Rigid Connections*, CRC Press, Boca Raton, FL, USA.

Fontana (2004), *Prescrizioni Tecniche*, s.l.: s.n.

Girão Coelho, A.M., Bijlaard, F. and Simoes Da Silva, L. (2004a), "Experimental assessment of the ductility of extended end plate connections", *Eng. Struct.*, **26**(9), 1185-1206.

Girão Coelho, A.M.G., da Silva, L.S. and Bijlaard, F.S.K. (2004b), "Characterization of the nonlinear behavior of single bolted T-tub connections", *Connections in Steel Structures V*, Amsterdam, The Netherlands, pp. 53-64.

Hantouche, E. and Abboud, N. (2014), "Stiffness modeling of bolted thick built-up T-stub connections including secondary prying effect", *J. Construct. Steel Res.*, **95**, 279-289.

Hantouche, E., Kukreti, A. and Rassati, G. (2012a), "Investigation of secondary prying in thick built-up T-stub connections using nonlinear finite element modeling", *Eng. Struct.*, **36**, 113-122.

Hantouche, E., Kukreti, A., Rassati, G. and Swanson, J. (2012b), "Built-up T-stub connections for moment resisting frames: Experimental and finite element investigation for prequalification", *Eng. Struct.*, **43**, 139-148.

Hantouche, E., Kukreti, A., Rassati, G. and Swanson, J. (2013), "Modified stiffness model for thick flange in built-up T-stub connections", *J. Construct. Steel Res.*, **81**, 76-85.

Hu, J., Leon, R. and Park, T. (2012), "Mechanical models for the analysis of bolted T-stub connections under cyclic loads", *J. Construct. Steel Res.*, **78**, 45-57.

Iannone, F., Latour, M., Piluso, V. and Rizzano, G. (2011), "Experimental analysis of bolted steel beam-to-column connections: Component identification", *J. Earthq. Eng.*, **15**(2), 214-244.

Jaspart, J. (1991), "Etude de la Semi-rigidite Des Noeuds Poutre-Colonne et son Influence sur la Resistance et la Stabilite des Ossature en Acier", Ph.D. Tesis; University of Liege, Liege, Belgium.

Kulak, G., Fisher, J. and Struik, J. (1987), *Guide to Design Criteria for Bolted and Riveted Joints*, John Wiley & Sons.

Latour, M. and Rizzano, G. (2013), "A theoretical model for predicting the rotational capacity of steel base joints", *J. Construct. Steel Res.*, **91**, 88-99.

Latour, M., Piluso, V. and Rizzano, G. (2011a), "Cyclic modeling of bolted beam-to-column connections: Component approach", *J. Earthq. Eng.*, **15**(4), 537-563.

Latour, M., Piluso, V. and Rizzano, G. (2011b), "Experimental analysis of innovative dissipative bolted double split tee beam-to-column connections", *Steel Construct.*, **4**(2), 53-64.

Latour, M., Piluso, V. and Rizzano, G. (2014), "Rotational behaviour of column base plate connections: Experimental analysis and modelling", *Eng. Struct.*, **68**, 14-23.

Lemonis, M.E. and Gantes, C.J. (2006), "Incremental modeling of T-stub connections", *J. Mech. Mater. and Struct.*, **1**(7), 1135-1159.

Leon, R. and Swanson, J. (2000), "Bolted steel connections: Tests on T-stub components", *J. Struct. Eng.*, **126**(1), 50-56.

Malvern, L. (1969), *Introduction of the Mechanics of the Continuous Medium*, Prentice-Hall, NJ, USA.

Nair, R.S., Birkemoe, P.C. and Munse, W.H. (1974), "High strength bolts subject to tension and prying", *J. Struct. Div.*, ASCE, **100**(2), 351-372.

Piluso, V. and Rizzano, G. (2008), "Experimental analysis and modelling of bolted T-stubs under cyclic loads", *J. Construct. Steel Res.*, **64**(6), 655-669.

Piluso, V., Faella, C. and Rizzano, G. (2001), "Ultimate behavior of bolted T-stubs. Part I: Theoretical model", *J. Struct. Eng. ASCE*, **127**(6), 686-693.

Pozzati, P. (1980), *Teoria e Tecnica delle strutture*, UTET, Torino, Italy.

Reinosa, J., Loureiro, A., Gutierrez, R. and Lopez, M. (2013), "Analytical frame approach for the axial stiffness prediction of preloaded T-stubs", *J. Construct. Steel Res.*, **90**, 156-163.

RILEM (1990), "Draft recommendation - Tension testing of metallic structural materials for determining stress-strain relations under monotonic and uniaxial tensile loading", *Mater. Struct.*, **23**(1), 35-46.

Saberi, V., Gerami, M. and Kheyroddin, A. (2014), "Comparison of bolted end plate and T-stub connection sensitivity to component thickness", *J. Construct. Steel Res.*, **98**, 134-145.

Swanson, J. (1999), "Characterization of the strength, stiffness and ductility behavior of T-stub connections", Ph.D. Thesis; Georgia Institute of Technology.

Swanson, J. (2002), "Ultimate strength prying models for bolted T-stub connections", *Eng. J.*, **3**, 136-147.

Swanson, J. and Leon, R. (2001), "Stiffness modeling of bolted T-stub connection components", *J. Struct. Eng.*, **127**(5), 498-505.

Takhirov, S.M. and Popov, E.P. (2002), "Bolted large seismic steel beam-to-column connections Part 2: Numerical nonlinear analysis", *Eng. Struct.*, **43**(12), 1535-1545.

Yee, Y. and Melchers, R. (1986), "Moment-rotation curves for bolted connections", *J. Struct. Eng. ASCE*, **112**(3), 615-635.

Zoetemeijer, P. (1974), "A design method for the tension side of statically loaded, bolted beam-to-column connections", *Heron*, **20**(1), 1-59.

CC

Annex A

The basic formulations for computing plastic rotations can be obtained with reference to the simple cantilever scheme depicted in Fig. 7. Four cases can be identified as follows:

Case 1: $\xi \le \xi_1 = \dfrac{M_y}{M_u}$

$$\vartheta_p = 0 \tag{1a}$$

Case 2: $\xi_1 < \xi \le \xi_2 = \dfrac{M_h}{M_u}$

The rotation corresponding to the attainment of the bending moment ξM_u can be evaluated through the following relationship

$$\vartheta = \int_0^L \chi(z)\,dz = \chi_\xi L - \int_0^{\chi_\xi} z(\chi)\,d\chi \tag{2a}$$

where χ_ξ is the curvature corresponding to the bending moment ξM_u.
Taking into account that

$$z(\chi) = \frac{M(\chi)}{\xi M_u} L = \frac{M(\chi)}{M_y} L_y \tag{3a}$$

the following relationship is attained

$$\int_0^{\chi_\xi} z(\chi)\,d\chi = L_y \int_0^{\chi_\xi} \frac{M(\chi)}{M_y}\,d\chi = \frac{\chi_y L_y}{2}\left(1 + C_{1,\xi}\right) \tag{4a}$$

where the coefficient $C_{1,\xi}$ is given by

$$C_{1,\xi} = \frac{\displaystyle\int_{\chi_y}^{\chi_\xi} z(\chi)\,d\chi}{\dfrac{\chi_y L_y}{2}} = \frac{1}{\chi_y}\int_{\chi_y}^{\chi_\xi}\left[3 - \left(\frac{\chi_y}{\chi}\right)^2\right]d\chi = 3\frac{\chi_\xi}{\chi_y} + \frac{\chi_y}{\chi_\xi} - 4 \tag{5a}$$

The rotation corresponding to the occurrence of the first yielding is given by $\vartheta_y = \dfrac{\chi_y L}{2}$; therefore, the plastic rotation is given by

$$\vartheta_p = \vartheta - \vartheta_y = \vartheta - \frac{\chi_y L}{2} \tag{6a}$$

By combining Eq. (6a) with Eqs. (2a), (4a) and (5a), the plastic rotation ϑ_p can be computed

$$\vartheta_p = \vartheta - \vartheta_y = \frac{\chi_y L}{2}\left[2\frac{\chi_\xi}{\chi_y} - \frac{1}{\xi}\frac{M_y}{M_u}\left(3\frac{\chi_\xi}{\chi_y} + \frac{\chi_y}{\chi_\xi} - 3\right) - 1\right] = \frac{L}{t_f}D(\xi) \tag{7a}$$

$$D(\xi) = \varepsilon_y \left[2\frac{\chi_\xi}{\chi_y} - \frac{1}{\xi}\frac{M_y}{M_u}\left(3\frac{\chi_\xi}{\chi_y} + \frac{\chi_y}{\chi_\xi} - 3\right) - 1 \right] \tag{8a}$$

where χ_ξ = function of ξ.

Obviously, for $\xi = \xi_2$ (which corresponds to $\chi_\xi = \chi_h$), the function $D(\xi)$ provides a value $D(\xi_2)$ that depends on the material properties only.

Case 3: $\xi_2 < \xi \le \xi_3 = \dfrac{M_m}{M_u}$

In this case, the rotation corresponding to the attainment of the bending moment ξM_u can still be evaluated using the Eq. (2a) considering that

$$\int_0^{\chi_\xi} z(\chi)\,d\chi = L_y\int_0^{\chi_\xi}\frac{M(\chi)}{M_y}\,d\chi = \frac{\chi_y L_y}{2}\left(1 + C_1 + C_{2,\xi}\right) \tag{9a}$$

where the coefficient C_1 is given by the Eq. (5a) with $\chi_\xi = \chi_h$; and the coefficient $C_{2,\xi}$ is given by

$$C_{2,\xi} = \frac{\displaystyle\int_{\chi_h}^{\chi_\xi} z(\chi)\,d\chi}{\dfrac{\chi_y L_y}{2}} = \frac{1}{\chi_y}\left\{\int_{\chi_h}^{\chi_\xi}\left[3 - \left(\frac{\chi_y}{\chi}\right)^2\right]d\chi + \frac{E_h}{E}\int_{\chi_h}^{\chi_\xi}\frac{\chi - \chi_h}{\chi_y}\left(1 - \frac{\chi_h}{\chi}\right)\left(2 + \frac{\chi_h}{\chi}\right)d\chi\right\} =$$
$$= \frac{\chi_h\left(3\chi_\xi^2 + \chi_y^2\right) - \chi_\xi\chi_y^2 - 3\chi_h^2\chi_\xi}{\chi_y\chi_h\chi_\xi} + \frac{E_h}{E}\frac{\left(\chi_\xi - \chi_h\right)^3}{\chi_\xi\chi_y^2} \tag{10a}$$

The plastic rotation can be still computed by means of Eq. (6a) so that, combining Eqs. (6a), (2a), (9a) and (10a), the plastic rotation ϑ_p can be computed

$$\vartheta_p = \vartheta - \vartheta_y = \frac{L\chi_y}{2}\left[2\frac{\chi_\xi}{\chi_y} - \frac{1}{\xi}\frac{M_y}{M_u}\left(3\frac{\chi_\xi}{\chi_y} + \frac{\chi_y}{\chi_\xi} - 3 + \frac{E_h}{E}\frac{\left(\chi_\xi - \chi_h\right)^3}{\chi_\xi\chi_y^2}\right) - 1\right] = \frac{L}{t_f}F(\xi) \tag{11a}$$

where

$$F(\xi) = \varepsilon_y\left[2\frac{\chi_\xi}{\chi_y} - \frac{1}{\xi}\frac{M_y}{M_u}\left(3\frac{\chi_\xi}{\chi_y} + \frac{\chi_y}{\chi_\xi} - 3 + \frac{E_h}{E}\frac{\left(\chi_\xi - \chi_h\right)^3}{\chi_\xi\chi_y^2}\right) - 1\right] \tag{12a}$$

Obviously, for $\xi = \xi_3$ (which corresponds to $\chi_\xi = \chi_m$), the function $F(\xi)$ provides a value $F(\xi_3)$ that depends on the material properties only.

Case 4: $\xi_3 < \xi \le 1$

In this case, the rotation θ can still be evaluated using the Eq. (2a), considering that

$$\int_0^{\chi_\xi} z(\chi)\,d\chi = L_y \int_0^{\chi_\xi} \frac{M(\chi)}{M_y}\,d\chi = \frac{\chi_y L_y}{2}\left(1 + C_1 + C_2 + C_{3,\xi}\right) \tag{13a}$$

where C_2 = value of $C_{2,\xi}$ for $\chi_\xi = \chi_m$; and the coefficient $C_{3,\xi}$ is given by

$$C_{3,\xi} = \frac{\displaystyle\int_{\chi_m}^{\chi_\xi} z(\chi)\,d\chi}{\dfrac{\chi_y L_y}{2}} = \frac{1}{\chi_y}\left\{\int_{\chi_m}^{\chi_\xi}\left[3 - \left(\frac{\chi_y}{\chi}\right)^2\right]d\chi + \frac{E_h}{E}\int_{\chi_m}^{\chi_\xi}\frac{\chi - \chi_h}{\chi_y}\left(1 - \frac{\chi_h}{\chi}\right)\left(2 + \frac{\chi_h}{\chi}\right)d\chi + \right.$$
$$\left. - \frac{E_h - E_u}{E}\int_{\chi_m}^{\chi_\xi}\frac{\chi - \chi_m}{\chi_y}\left(1 - \frac{\chi_m}{\chi}\right)\left(2 + \frac{\chi_m}{\chi}\right)d\chi\right\} \tag{14a}$$

By solving the integrals, the Eq. (14a) can be simplified

$$C_{3,\xi} = \frac{\chi_m\left(3\chi_\xi^2 + \chi_y^2\right) - \chi_\xi\chi_y^2 - 3\chi_m^2\chi_\xi}{\chi_y\chi_m\chi_\xi} - \frac{E_h - E_u}{E}\frac{\left(\chi_\xi - \chi_m\right)^3}{\chi_\xi\chi_y^2} +$$
$$+ \frac{E_h}{E}\frac{\chi_h^3\left(\chi_\xi - \chi_m\right) - 3\chi_h\chi_m\chi_\xi\left(\chi_\xi - \chi_m\right) + \chi_m\chi_\xi\left(\chi_\xi^2 - \chi_m^2\right)}{\chi_\xi\chi_m\chi_y^2} \tag{15a}$$

Finally, combining Eqs. (6a), (2a), (13a) and (15a), the plastic rotation ϑ_p is given by

$$\vartheta_p = \vartheta - \vartheta_y = \frac{\chi_y L}{2}\left[2\frac{\chi_\xi}{\chi_y} - \frac{1}{\xi}\frac{M_y}{M_u}\left(3\frac{\chi_\xi}{\chi_y} + \frac{\chi_y}{\chi_\xi} - 3 + \frac{E_h}{E}G_h + \frac{E_u}{E}G_u\right) - 1\right] = \frac{L}{t_f}G(\xi) \tag{16a}$$

where

$$G(\xi) = \varepsilon_y\left[2\frac{\chi_\xi}{\chi_y} - \frac{1}{\xi}\frac{M_y}{M_u}\left(3\frac{\chi_\xi}{\chi_y} + \frac{\chi_y}{\chi_\xi} - 3 + \frac{E_h}{E}G_h + \frac{E_u}{E}G_u\right) - 1\right] \tag{17a}$$

with

$$G_h = \frac{\chi_m^3}{\chi_\xi\chi_y^2} + 3\frac{\chi_\xi\chi_m}{\chi_y^2} - 3\frac{\chi_m^2}{\chi_y^2} + 3\frac{\chi_h^2}{\chi_y^2} - 3\frac{\chi_\xi\chi_h}{\chi_y^2} - \frac{\chi_h^3}{\chi_\xi\chi_y^2}$$

$$G_u = \frac{\chi_\xi^2}{\chi_y^2} + 3\frac{\chi_m^2}{\chi_y^2} - 3\frac{\chi_\xi\chi_m}{\chi_y^2} - \frac{\chi_m^3}{\chi_\xi\chi_y^2} \tag{18a}$$

Obviously, for $\xi = 1$ (which corresponds to $\chi_\xi = \chi_u$), the function $G(\xi)$ provides a value $C = G(1)$ that depends on the material properties only.

Annex B

With reference to the scheme in Fig. 12, the expressions of the displacements has been computed by dividing the plate in three parts and writing the static beam equations
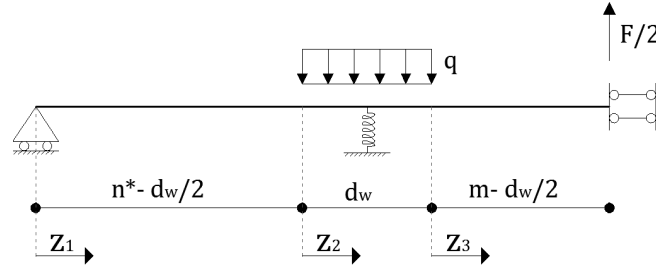

Fig. 12 Static scheme for the evaluation of the elastic displacements

For $0 \leq z_1 \leq n^* - \dfrac{d_w}{2}$

$$v_1(z_1) = -\frac{2Fz_1\left[-3\left(m+n^*\right)^2 + z_1^2\right] - qd_wz_1\left\{d_w^2 + 4\left[z_1^2 - 3n^*\left(2m+n^*\right)\right]\right\}}{24EI} \tag{1b}$$

For $0 \leq z_2 \leq d_w$

$$\begin{aligned}
v_2(z_2) = -\frac{1}{96EI}\Big\{ &4qd_w^4 - d_w^3\left[F + 16q\left(n^*+z_2\right)\right] + \\
&+ 4\left[qz_2^4 - 2F\left(n^*+z_2\right)\left(3m^2 + 6mn^* + 2n^{*2} - 2n^*z_2 - z_2^2\right)\right] + \\
&+ 4d_w\left[3F\left(m-z_2\right)\left(m+2n^*+z_2\right) + 4q\left(n^*+z_2\right)\right]\left[2n^*\left(3m+n^*\right) - 2n^*z_2 - z_2^2\right] + \\
&+ 6d_w^3\left[F\left(n^*+z_2\right) + 4q\left(-2mn^* + 2n^*z_2 + z_2^2\right)\right]\Big\}
\end{aligned} \tag{2b}$$

For $0 \leq z_3 \leq m - \dfrac{d_w}{2}$

$$\begin{aligned}
v_3(z_3) = -\frac{1}{96EI}\Big\{ &d_w^3\left(F - 16qn^*\right) - 8F\left(n^*+z_3\right)\left(3m^2 + 6mn^* + 2n^{*2} - 2n^*z_3 + z_3^2\right) + \\
&+ 6d_w^2\left[8qn^*\left(m-z_3\right) + F\left(n^*+z_3\right)\right] + \\
&+ 4d_w\left\{-3F\left(m-z_3\right)\left(m+2n^*+z_3\right) + 4qn\left[2n^{*2} - 3z_3^2 + 6m\left(n^*+z_3\right)\right]\right\}\Big\}
\end{aligned} \tag{3b}$$

where F is the load level, q is the bolt action, E is the Young modulus, I the inertial moment of the bolt section, m, n^* and d_w are the geometrical parameters first shown.

Starting from the definition of the plate deflections it is possible also to determine the value of the $\delta_{b,el}$ to be used in Eq. (2.b) (by imposing $z_2 = d_w / 2$)

$$\delta_{b,el} = -\frac{qd_w^4 - 16n^*\left[2F\left(3m^2 + 6mn^* + 2n^{*2}\right) + qd_w^3 - 8qd_wn^*\left(3m+n^*\right)\right]}{384EI} \tag{4b}$$